

Increased seed number per silique in *Brassica juncea* by deleting *cis*-regulatory region affecting *BjCLV1* expression in carpel margin meristem

Gang Wang , Xiangxiang Zhang, Wei Huang, Ping Xu, Zewen Lv, Lun Zhao, Jing Wen , Bin Yi, Chaozhi Ma, Jinxing Tu , Tingdong Fu and Jinxiong Shen* 

National Key Laboratory of Crop Genetic Improvement/National Engineering Research Center of Rapeseed, Huazhong Agricultural University, Wuhan, China

Received 7 May 2021;

revised 24 June 2021;

accepted 11 July 2021.

*Correspondence (Tel +86 27 8728 0009;

fax +86 27 8728 0009;

email: jxshen@mail.hzau.edu.cn)

Summary

Mustard yield per plant is severely restricted by the seed number per silique. The seed number per silique in the *Brassica juncea* trilocular mutant J163-4 is significantly greater than that in normal bilocular plants. However, how the trilocular silique of J163-4 is formed remains unclear. Here, we studied the gene structure and function of *mc2* in *B. juncea* and *Arabidopsis* using comparative morphology and molecular genetic experiments. We found that *mc2* is a *CLV1* ortholog, *BjA7.CLV1*. The deletion of *cis*-regulatory region in *mc2* promoter, which affects *Mc2* expression in carpel margin meristem (CMM), led to trilocular silique formation. The *BjCLV1* sequence with its complete promoter containing the *cis*-regulatory region can restore the *Bjclv1* and *clv1* mutant phenotypes in *B. juncea* and *Arabidopsis*, respectively. Additionally, this *cis*-regulatory region had a collinear segment in the promoter of *CLV1* homologous gene in most Brassicaceae species. Our results are consistent with the report that *BjCLV1* represents a conserved pleiotropic role in shoot meristem and CMM development, which contains a *cis*-regulatory sequence specifically expressed *BjCLV1* in CMM in its promoter, and this *cis*-regulatory region is conserved in Brassicaceae species. These results offer a reliable approach for fine-tuning the traits of seed yield in Brassicaceae crops.

Keywords: *BjCLV1*, *Brassica juncea*, carpel margin meristem, Brassicaceae, trilocular silique, yield-related traits.

Introduction

Brassica juncea (*B. juncea*, AABB, 2n=36), one of the three most commonly planted rapeseeds worldwide, is widely used in the genetic improvement of *Brassica napus* as a donor resource. Many natural plant variants with multilocular siliques have been found for *B. juncea*. Its yield per plant is significantly higher than that of bilocular mustard, which has siliques with two locules, under the same genetic background, mainly due to the increased seed number per silique (Katiyar *et al.*, 1998; Lv *et al.*, 2012; Zhao *et al.*, 2003).

The silique of *B. juncea*, derived from the gynoeceum, typically comprises two fused carpels separated by two repla connected to a false septum, which divides the silique into two locules (bilocular) with two rows of seeds growing at the junction between the septum and replum. However, multilocular siliques comprise more than two fused carpels, and different false septa divide the silique into multiple locules, each containing more than one row of seeds. Genetic studies have indicated that the multilocular trait of the MVS7, MVS8 and MVS24 lines (Choudhary and Solanki, 2007), as well as the 'duoshi' cultivar (Xiao *et al.*, 2013), is controlled by two independently inherited recessive nuclear genes in *B. juncea*. *Arabidopsis* gynoeceum comprises two congenitally fused carpels that form a hollow tube (Smyth *et al.*, 1990). In early gynoeceum development, a tissue with meristematic identities forms along the margins where the carpels fuse, which is called carpel margin meristem (CMM) (Long *et al.*, 1996; Reyes-Olalde *et al.*, 2013). As development

proceeds, the CMM gives rise to medial tissues and organs, including the placenta, ovules, septum and transmitting tract (Bowman *et al.*, 1999).

Shoot meristems, including shoot apical meristem (SAM), inflorescence meristem (IM) and floral meristem (FM), are maintained by pluripotent stem cells that are controlled by classical CLAVATA (CLV)-WUSCHEL (WUS) feedback signalling established in *Arabidopsis* (Brand *et al.*, 2000; Schoof *et al.*, 2000) conserved in crops, such as maize, rice, tomato and rapeseed (Somssich *et al.*, 2016). This pathway relies on communication between peptide ligands, a series of receptors, and transcription factors (TFs) expressed in different zones and coordinate stem cell proliferation with differentiation. The cores of this complex network are WUS, a mobile homeodomain TF expressed in the organizing centre (OC) that can move to the central zone (CZ) to promote stem cell fate (Yadav *et al.*, 2011), especially by repressing differentiation (Mayer *et al.*, 1998) and CLV3 (Fletcher *et al.*, 1999), a small peptide ligand whose expression is induced by WUS in the CZ but can repress WUS expression when perceived by leucine-rich repeat receptor-like kinases (LRR-RLKs), such as CLV1 (Clark *et al.*, 1997), and a leucine-rich repeat receptor-like protein (LRR-RLP) CLV2 (Jeong *et al.*, 1999). Over the past 30 years, mutations in *CLV1* in *Arabidopsis* and *CLV1* orthologs in crops, such as the *CLV1* orthologs in rice (Suzaki *et al.*, 2004), in maize (Bommert *et al.*, 2005), in tomato (Xu *et al.*, 2015) and in *B. juncea* (Chen *et al.*, 2018; Xiao *et al.*, 2018), often created great interest, which contains enlarged shoot meristems, flattened stems and increased floral and fruit

organ number. However, despite mutations in *CLV1* and *CLV1* orthologs involved in shoot meristem activity that affect the formation of these gynoecial structures, little is known about their direct roles in CMM development.

J163-4, whose siliques exhibit a trilobular trait, is a landrace of *B. juncea*. Genetic studies have shown that the trilobular trait of J163-4 is controlled by a pair of recessive nuclear genes, *mc1* and *mc2* (Lv *et al.*, 2012), and mapping studies have delimited *mc2* to 68 kb in the Scaffold 000019 physical map of A7 in *Brassica rapa* (Wang *et al.*, 2016). In this study, we cloned another trilobular gene of J163-4, *mc2*. By studying the gene structure and function of *mc2* in *B. juncea* and *Arabidopsis* using comparative morphology and molecular genetic experiments, we report that a 914-bp deletion in *mc2* promoter, which contains a *cis*-regulatory sequence, specifically expressed *BjCLV1* in CMM, and this *cis*-regulatory region is conserved in Brassicaceae species. These findings offer a new and reliable approach for fine-tuning the traits of seed yield in Brassicaceae crops.

Results

mc2 mutation affects CMM size with increased yield

To specify the timing and phenotypic effects of *mc2* locus on chromosome A7 in *B. juncea*, near-isogenic lines BC₇F₂, homozygous for wild-type and mutant alleles, were used for comparative developmental studies. The most prominent phenotype of the *mc2* plants was in the development of siliques, which at maturity were abnormally flattened and wider than normal (Figure 1a–d), with four carpels and three loculi separated by an 'II'-type false septum (Figure 1f,h). Notably, *mc2* siliques can bear an average of 25 seeds (Figure 1f,h), versus 17 seeds for normal siliques (Figure 1e,g), without a reduction in the 1000-seed weight (Table 1), although they are shorter in length (Table 1), indicating that *mc2* plants have great potential for the future genetic improvement of yield traits in mustard (Table 1). The architecture of the *mc2* plants was relatively normal (Table 1) compared to that of siliques.

The near-isogenic lines were further compared in order to determine when *mc2* first affected meristem development. We found that *mc2* mainly affects gynoecium development but has no apparent effect on other tissues and organ development during the embryonic, vegetative seedling and early flowering stage (Figure S1). To further explore the potential effects of *mc2* on the early stages of gynoecium development, the early development of *mc2* gynoecium was examined using scanning electron microscopy (SEM). At stage 4 of flower development, the *mc2* flowers exhibited a normal phenotype (Figure 1i,n). However, when carpel primordia were initiated in the centre of FM, the difference between *mc2* and normal gynoecia could be seen at stage 5. At this stage, a tissue with meristematic identities called the CMM forms along the margins where the carpels fuse in the medial region of *mc2* gynoecia, which began to swell compared to normal gynoecia (Figure 1j,o). When the gynoecium began to develop as a raised ridge around a central cleft at stage 6, every enlarged CMM of *mc2* gynoecium developed into two CMMs (Figure 1p). The normal gynoecium comprises two congenitally fused carpels and two CMMs (Figure 1k), which arise as a cylinder-like structure because they are joined at the margins in the medial region (Figure 1l,m). In contrast, the *mc2* gynoecium comprised four acquired carpels and four CMMs, which arise as square-like structures (Figure 1q). This abnormal gynoecium was

more obviously distinct than that of the normal gynoecium at stage 8 (Figure 1r). Compared to those of gynoecia, the stature and number of other floral organs of the *mc2* flowers were relatively standard (Figure 1n–r).

To further investigate the potential effects of additional CMMs on gynoecium development in later stages, the development of internal tissues of *mc2* gynoecium was analysed by cross section. As CMM development proceeds, the septum is initiated during stage 8 when the inner medial surfaces form ridges (Figure 1s,v) and forms properly during stage 9 when the leading edges of each medial ridge meet and fuse (Figure 1t,w). At stage 12, normal CMMs gave rise to an 'I'-typed false septum and two rows of ovules (Figure 1u); however, the *mc2* CMMs gave rise to an 'II'-typed false septum and more than two rows of ovules (Figure 1x). These phenotypes were consistent with the observation that mature *mc2* siliques are composed of four carpels and three loci (Figure 1f,h).

To summarize, *mc2* plants were defective in regulating CMM size in early gynoecium phases and showed no apparent abnormalities in other meristems. The *mc2* siliques produced extra carpels, and seeds resulted from enlarged CMMs. Therefore, *mc2* plants can be defined as weak mutants.

Mc2 encodes *CLV1*, and a 914-bp deletion region exists in the *mc2* promoter

The *Mc2* gene was previously positioned in a region between markers ZX17 and BACsr96, which has perfect collinearity with a 68-kb physical region between 946 and 1014 kb in Scaffold 000019 physical map of A7 in *B. rapa* (Wang *et al.*, 2016). Subsequently, the full-length sequencing of two positive clones of a purple-leaf mustard BAC library, 002-O-21 and 009-M-2, screened by the flanking markers linked to *Mc2*, was completed, and three contigs (designated as contig 1, 2, and 3) were obtained. Using BLAST, the physical positions of the markers ZX17 and BACsr96 in contig 1 were found to be 89.5 and 54.6 kb, respectively (Figure 2a), covering a physical interval of 34.9 kb. When the whole genome sequencing of *B. juncea* was completed (Yang *et al.*, 2016), markers ZX17 and BACsr96 were aligned at the physical positions of 32 935 and 32 900 kb on Chr.A07, respectively (Figure 2a), indicating that the previous localization results of *Mc2* were reliable. Notably, this genomic region contains only six annotated open reading frames, including a homolog of *Arabidopsis thaliana* *CLAVATA1* (*CLV1*, At1g75820), *BjA7.CLV1* (*BjuA029486*) (Figure 2b; Table S1). Given that *clv1* mutants could increase flower organ numbers, especially carpels (Clark *et al.*, 1993), it is reasonable to speculate that *BjA7.CLV1* is a candidate gene for *Mc2*.

To confirm the candidate gene for *Mc2* loci, a series of gene-specific primers for amplifying *BjA7.CLV1* in bilobular and trilobular parents were designed based on the contig 1 sequence. Compared to the sequencing results, the CDS (3043 bp) and 3'-UTR (1248 bp) regions of *BjA7.CLV1* showed no difference in the bilobular and trilobular parents, but a 914-bp deletion was identified in the regulatory region –2865 bp upstream of *BjA7.CLV1* in J163-4 (Figure 2c). These results show that *BjA7.CLV1* is a reliable candidate gene for *Mc2*.

BLAST searching BRAD database revealed that *CLV1* is highly conserved in brassicaceous species and contains at least one homologous copy (Figure 2d). *Brassica* allotetraploids, such as *B. juncea* and *B. napus*, have two *CLV1* homologs (Figure 2d).

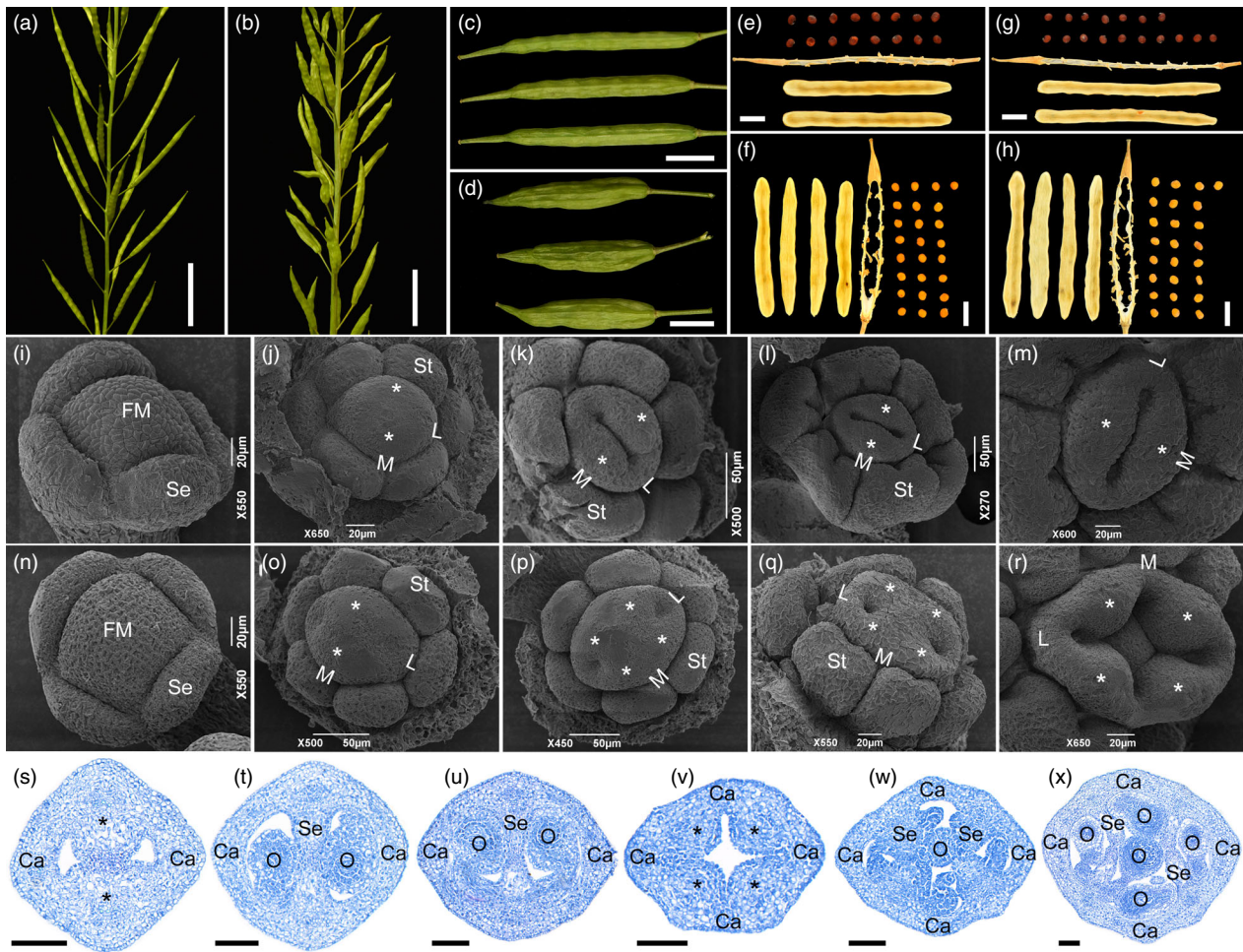


Figure 1 Phenotype of bilocular and trilocular plants in A-Bi and A-Tri lines. (a) Bilocular plant. (b) Trilocular plant. (c) Bilocular silique. (d) Trilocular silique. (e, g) Mature silique with two valves and an 'I'-shaped false septum from J268-1 and A-Bi. (f, h) Mature silique with four valves and an 'II'-shaped false septum from J163-4 and A-Tri. (i–r) Scanning electron microscopy of bilocular and trilocular flowers. (i) Stage 3 bilocular flower. (j) Stage 5 bilocular flower with sepal removed. (k) Stage 6 bilocular flower. (l) Stage 7 bilocular flower. (m) Stage 7 bilocular gynoecium in (l). (n) Stage 3 trilocular flower. (o) Stage 5 trilocular flower. Note: the gynoecium at this stage shows the abnormality at the CMMs. (p) Stage 6 trilocular flower. (q) Stage 7 trilocular flower. (r) Stage 8 trilocular gynoecium. (s–x) Cross sections for analysing the development of internal tissues of the gynoecium. (s) Stage 8 section of a bilocular plant. (t) Stage 10 section of a bilocular plant. (u) Stage 12 section of a bilocular plant. (v) Stage 8 section of a trilocular plant. (w) Stage 10 section of a trilocular plant. (x) Stage 12 section of a trilocular plant. FM, floral meristem; Se, sepal; St, stamen; M, medial region; L, lateral region; *, carpel margin meristem (CMM); Ca, Carpel; Se, septum; O, ovule. Scale bars = 3 cm for (a) and (b), 1 cm for (c) and (d), 0.5 cm for (e–h), and 100 μ m for (s–x).

Phylogenetic analysis showed that *Brassica CLV1* genes were assigned to subclades following their localization to the A, B or C subgenomes (Figure 2d). *BjA7.CLV1* (*Mc2*) has high homology with *BraCLV1* derived from *B. rapa*, whereas *BjB3.CLV1* (*Mc1*) has high homology with *BniCLV1* derived from *B. nigra* (Figure 2d).

To further understand whether the 914-bp deletion sequence of the *mc2* promoter was similarly conserved in the promoter region of these homologous genes, BLAST analysis using the 914-bp deletion sequence as a query was performed in the BRAD database. Conservatory analysis showed that the 914-bp deletion sequence of the *mc2* promoter had a relatively high level of conservation, especially in *Brassica* species, with 602-bp and 282-bp sequences conserved within *Mc1* and *AtCLV1*, respectively (Figure 2d).

Trilocular siliques are formed owing to the 914-bp regulatory sequence deletion in the promoter

Real-time quantitative PCR analysis revealed no significant difference in the expression of *Mc2* transcripts in the seedling-stage young leaves and inflorescences of *pMc2::Mc2* and *pmc2::Mc2* transgenic plants (Figure 3b); however, there was a significant difference in the ovary (Figure 3b). Similarly, *Mc1* transcripts in *pMc1::Mc1* and *pmc1::Mc1* transgenic plants only showed significant differences in expression in the ovary (Figure 3a). Cross-sectional analysis results showed that *p35S::Mc1* (Figure 3c), *pMc1::Mc1* (Figure 3d), *p35S::Mc2* (Figure 3f) and *pMc2::Mc2* (Figure 3g) transgenic plants could restore the bilocular silique phenotype composed of two carpels and an 'I'-typed septum (Figure 3c), while *pmc2::Mc2*

Table 1 Descriptive statistics of the traits

Combinations	Genotype	Plant height (cm)	Number of primary branches	Number of siliques per plant	Silique length (cm)	Silique body length (cm)	Seeds per silique	Thousand seed weight (g)	Seed yield per plant (g)
J248-2 × J163-4	B-Bi: <i>Mc1Mc1mc2mc2</i>	250.4 ± 4.92	7.3 ± 0.59	516.1 ± 18.6	3.87 ± 0.62*	3.16 ± 0.21*	13.8 ± 0.81	2.11 ± 0.11	12.21 ± 0.79
	B-Tri: <i>mc1mc1mc2mc2</i>	251.2 ± 3.24	7.5 ± 0.67	503.5 ± 11.4	3.18 ± 0.62	2.37 ± 0.23	21.3 ± 1.24*	2.07 ± 0.13	16.72 ± 0.94*
J268-1 × J163-4	A-Bi: <i>mc1mc1Mc2Mc2</i>	271.5 ± 3.39	7.6 ± 0.62	533.2 ± 15.7	4.15 ± 0.62*	3.24 ± 0.19*	16.7 ± 0.75	2.25 ± 0.11	15.55 ± 0.67
	A-Tri: <i>mc1mc1mc2mc2</i>	270.9 ± 2.75	7.8 ± 0.86	522.2 ± 27.5	3.51 ± 0.15	2.74 ± 0.12	25.4 ± 0.97*	2.18 ± 0.12	22.07 ± 1.23*

Data and errors bars represent mean ± SD.

*Significant at 1% level.

(Figure 3e) and *pmc1::Mc1* (Figure 3h) transgenic plants could not restore the bilocular silique phenotype, and those silique is composed of four carpels and an 'II'-typed septum or three carpels and a 'Y'-typed septum. The silique phenotype of mature plants can also be seen in *p35S::Mc2* (Figure 3i), *pMc2::Mc2* (Figure 3j), *p35S::Mc1* (Figure 3l) and *pMc1::Mc1* (Figure 3m) transgenic plants, which are mainly composed of bilocular siliques (Figure S3), whereas *pmc2::Mc2* and *pmc1::Mc1* transgenic plants are mainly composed of trilocular siliques (Figure 3k,n, S3). Four constructs (*pMc2::Mc2*, *pmc2::Mc2*, *pMc1::Mc1* and *pmc1::Mc1*) were transformed into *Arabidopsis clv1-1* mutants [*clv1-1*, which produce siliques with four carpels (Clark *et al.*, 1993; Clark *et al.*, 1997)]. We found that *pMc1::Mc1* and *pMc2::Mc2* transgenic plants could restore the bilocular silique phenotype, while *pmc2::Mc2* and *pmc1::Mc1* transgenic plants could not restore the bilocular silique phenotype (Figure S4), but the number of seeds per trilocular silique of *pmc2::Mc2* and *pmc1::Mc1* transgenic plants was more than that of *Ler* and *clv1-1*, and *pmc2::Mc2* and *pmc1::Mc1* transgenic plants exhibited a similar stature phenotype to those of normal plants (Figure S4).

In summary, constructs lacking this 914-bp region in *mc1* and *mc2* promoters only affected the development of CMMs in *B. juncea* or *Arabidopsis* and do not affecting the development of other tissues and organs, which reflected increased number of carpels and locules and space of ovary, ultimately leading to an increase in the number of seeds per silique.

The 914-bp regulatory sequence deletion in the promoter affects *Mc2* transcript expression in the gynoecial CMMs

To evaluate the expression patterns of *Mc1* and *Mc2*, tissues from the NILs B-BC₆F₂ and A-BC₇F₂, homozygous for wild-type and mutant alleles, were carried out qRT-PCR analyses. The results showed that *Mc1* transcripts were strongly expressed in the roots, buds and ovaries derived from B-Bi plants, followed by those in the stems, leaves and inflorescences (Figure 4a). However, *Mc1* transcripts were not detected in the *mc1* plants because RTE1 in the coding region of *Mc1* interrupted its transcription (Figure 4a) (Xu *et al.*, 2017). *Mc2* transcripts had the highest expression in the bud and root derived from A-Bi and *mc2* plants, followed by that in the stem, leaf and inflorescence, and there was no significant difference in expression (Figure 4b). However, *Mc2* transcripts showed significant expression differences in the ovaries of A-Bi- and *mc2*-derived plants (Figure 4b).

To determine whether the 914-bp deletion sequence of the *mc2* promoter and collinearity segments of the 914-bp deletion sequence in the *Mc1* promoter could affect the expression pattern of *Mc2* and *Mc1*, we examined the promoter activity of *Mc1* and *Mc2* using transgenic *Arabidopsis* expressing GUS gene under the control of full-length or truncated promoters. Consistent with the qRT-PCR analyses, GUS activity was detected in most tissues and organs investigated when controlled by the full-length promoters (Figure 4c,e, S5), while it was not detected in CMM of gynoecium controlled by the truncated promoters (Figure 4d,f). These results suggest that *Mc1* and *Mc2* play vital roles in various tissues and organs of *B. juncea* and that the 914-bp deletion region of the *mc2* promoter and its collinearity segments in the *Mc1* promoter contain *cis*-regulatory elements that are crucial for *Mc2* and *Mc1* expression in CMM.

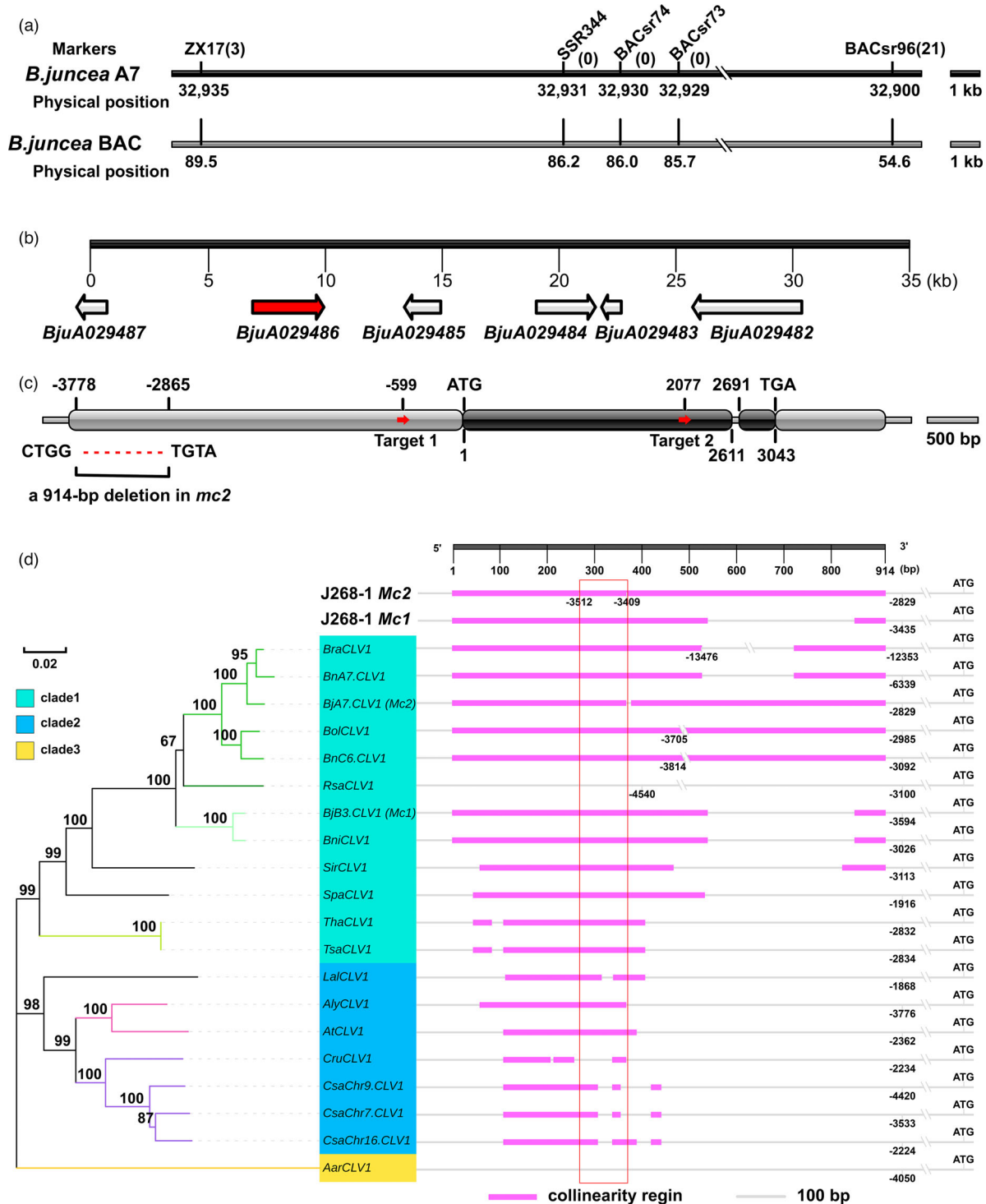


Figure 2 Molecular characterization of the *Mc2* gene. (a) Fine mapping of the *Mc2* gene to a 35-kb region between the markers ZX17 and BACsr96 of chromosome A7. The numbers in parentheses indicate the number of recombinants of corresponding markers. The grey physical map below represents the corresponding purple-leaf mustard *Brassica juncea* BAC clone 002-O-21 and 009-M-2 region homologous to the region in which *Mc2* resides. (b) The refined 35-kb region at the *Mc2* locus contained six annotated genes, and the red arrow represents the candidate gene *Mc2*. (c) Gene structure of the candidate gene and polymorphisms between the two parents. Dark grey columns represent exons, and light grey columns represent the promoter and 3'-flanking region. The red dashed line represents a 914-bp deletion in *mc2*. The two red arrowheads indicate two single gRNA target sites for CRISPR/Cas9. (d) Phylogenetic tree and promoter conservatory analysis of *Mc2* and homologous genes in the Brassicaceae family. The neighbour-joining phylogenetic tree was constructed using MEGA X. The numbers at the nodes represent percentage bootstrap values based on 1000 replicates. The lengths of the branches refer to the nucleotide variation rates. The red box represents the core region that may contain *cis*-regulatory elements specifically expressed in the carpel margin meristem (CMM).

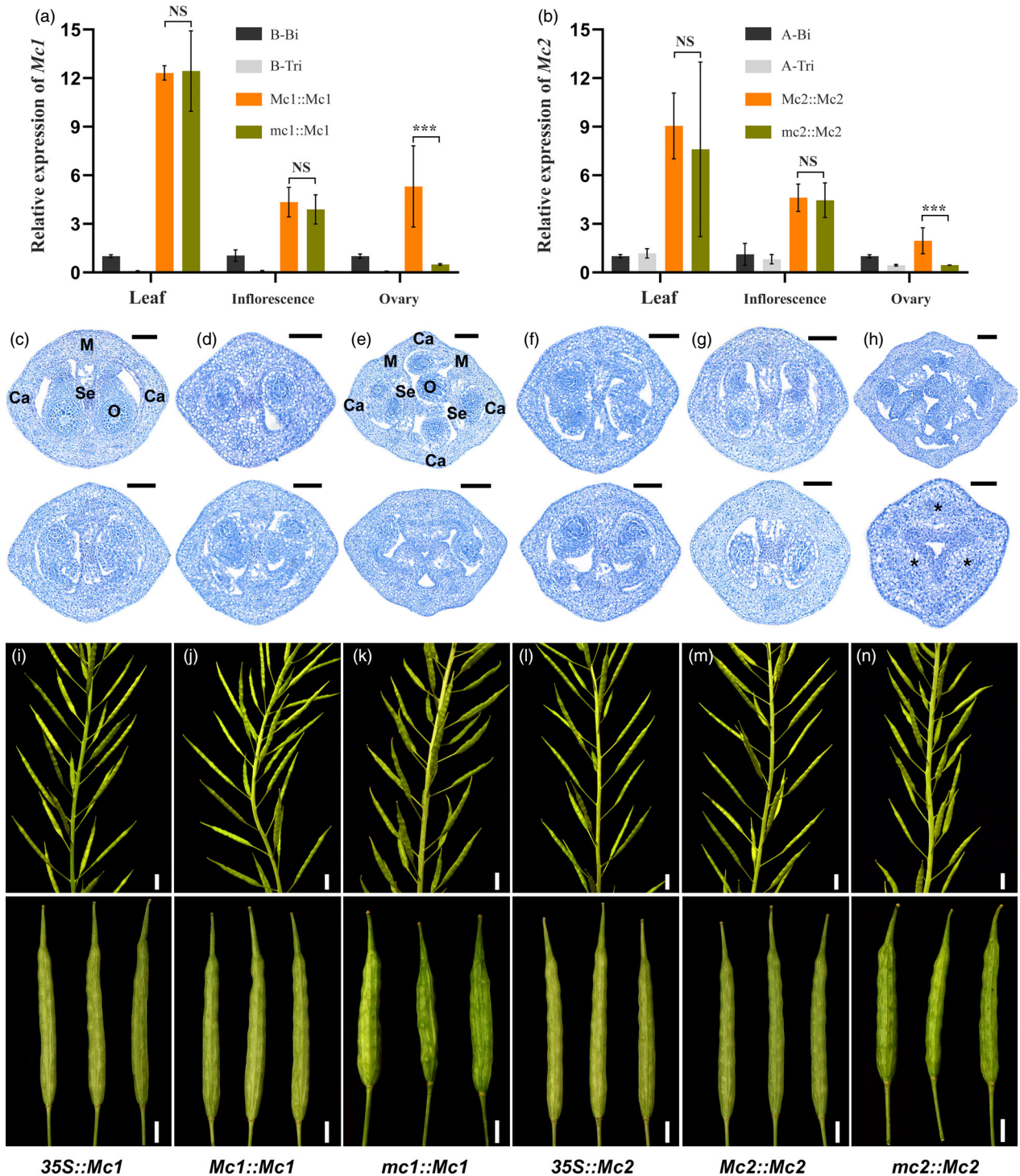


Figure 3 Complementation test and overexpression of *Mc1* and *Mc2* in *Brassica juncea*. (a, b) Expression of *Mc1* (a) and *Mc2* (b) in different tissues of T₁ transgenic lines, as revealed by quantitative RT-PCR. Error bars indicate SD of three replicates. (c–n) Cross sections to analyse the development of internal tissues of the gynoceium. (c, d) Stage 12 section of *p35S::Mc1*. (e, f) Stage 12 section of *pMc1::Mc1*. (g, h) Stage 12 and 10 sections of *pmc1::Mc1*, respectively. (i, j) Stage 12 section of *p35S::Mc2*. (k, l) Stage 12 and 11 sections of *pMc2::Mc2*, respectively. (m, n) Stage 10 and 8 sections of *pmc2::Mc2*, respectively. (o–z) T₁ Phenotypes of plant complementation test and overexpression. (o, u) Plant and siliques of *p35S::Mc1*. (p, v) Plant and siliques of *pMc1::Mc1*. (q, w) Plant and siliques of *pmc1::Mc1*. (r, x) Plant and siliques of *p35S::Mc2*. (s, y) Plant and siliques of *pMc2::Mc2*. (t, z) Plant and siliques of *pmc2::Mc2*. M, medial region; Ca, carpel; Se, septum; O, ovule; *, carpel margin meristem (CMM). Scale bars = 100 μm for (c–n), 1 cm for (o–t) and 0.5 cm for (u–z). Significant differences by Student’s *t*-test are shown as NS, not significant at $P \geq 0.05$; *** $P < 0.001$.

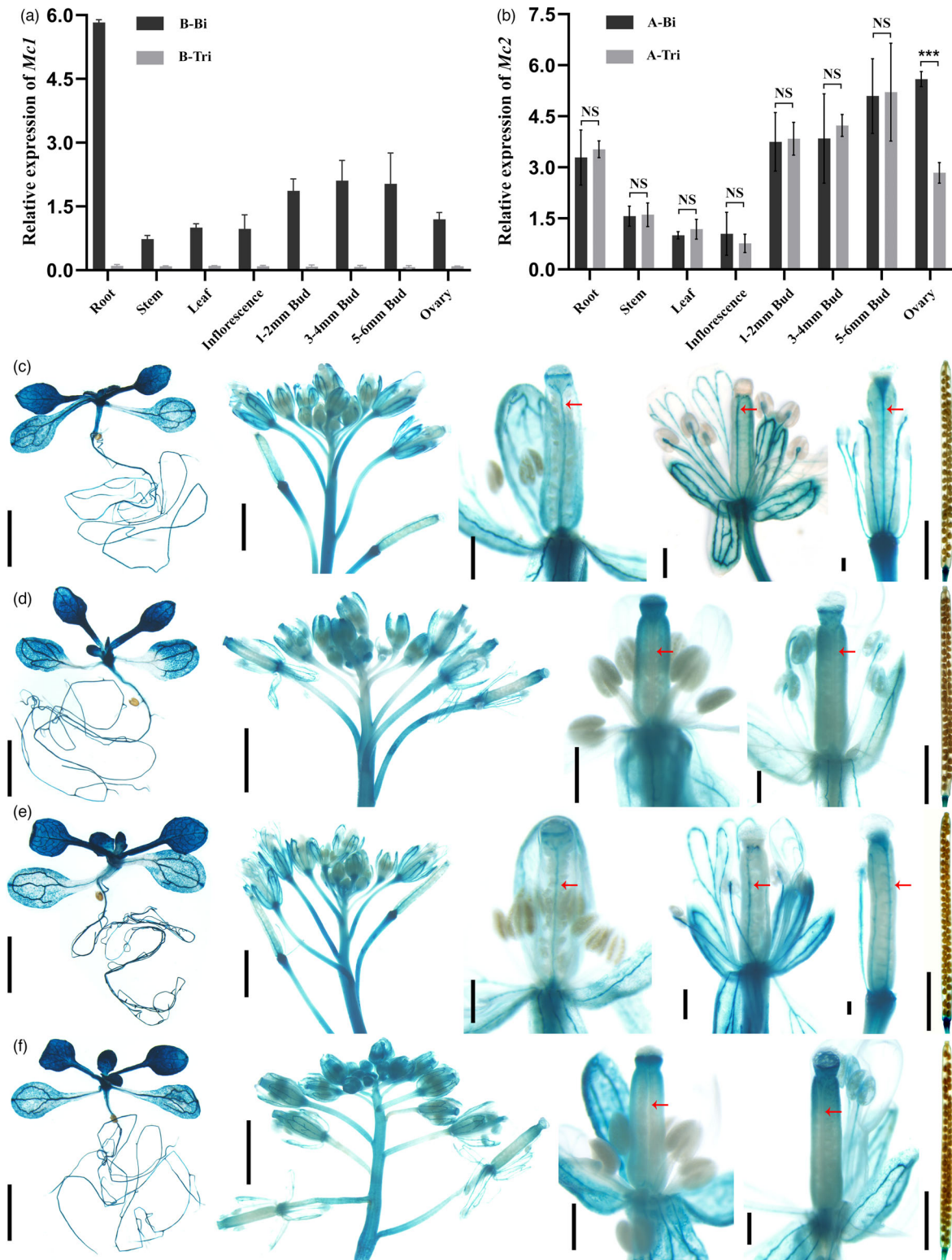


Figure 4 Expression pattern of *Mc1* and *Mc2*. (a) Expression of *Mc1* in various tissues from B-Bi and B-Tri detected using qRT-PCR. (b) Expression of *Mc2* in various tissues from A-Bi and A-Tri detected using qRT-PCR. Error bars in (a) and (b) represent SD from three biological replicates. Significant differences by Student's *t*-test are shown as NS, not significant at $P \geq 0.05$; *** $P < 0.001$. (c-f) GUS staining showing *Mc1* and *Mc2* expression in the carpal margin meristem (CMM) of *pMc1::GUS* (c) and *pMc2::GUS* (e) *Arabidopsis*, but no expression in the CMM of *pmc1::GUS* (d) and *pmc2::GUS* (f) *Arabidopsis*. Scale bars = 2.5 mm, 1 mm, 100 μ m, 100 μ m and 2 mm for (c) and (e) (from left to right) and 2.5 mm, 1 mm, 100 μ m, 100 μ m and 2 mm for (d) and (f) (from left to right).

–3512- to –3409-bp region of the *Mc2* promoter for expression of *Mc2* in CMM

To further identify the regulatory region for CMM-specific expression in the 914-bp deletion sequence, we studied the *GUS* reporter gene driven by a series of progressive 5'-deletion *Mc2* promoters in *Col*. The results of staining in flowers revealed an intense *GUS* activity in the CMM of gynoecium from three transgenic plants [GUS2-1 (–3631bp), GUS2-2 (–3562bp) and GUS2-3 (–3512bp)] (Figure 5a–c), while slight *GUS* staining was also detected in the CMM of GUS2-4 (–3468bp) (Figure 5d) gynoecium. However, *GUS* staining was not detected in the CMM of gynoecium of the other six constructs (Figure 5e–j). Additionally, *Mc2* gene expression was driven by different deletions of its native promoter (Figure S6) in which *clv1-1* mutant was studied. The phenotypic results showed that the Mc2G-1, Mc2G-2 and Mc2G-3 transgenic plants exhibited a similar stature phenotype and silique architecture to *Ler* (Figure 5a–c), and the average proportion of bilocular siliques per plant exceeded 98% (Figure 5k; Table S2), indicating that these plants recovered a bilocular phenotype. Mc2G-4 (Figure 5d) transgenic plants included part of tricarpetate siliques, the average proportion of which was less than 20% (Figure 5k; Table S2), indicating that these plants only partially recovered a bilocular phenotype. In contrast, the other six transgenic plants (Mc2G-5, Mc2G-6, Mc2G-7, Mc2G-8, Mc2G-9 and Mc2G-10) (Figure 5e–j) exhibited a similar stature phenotype and silique architecture to *pmc2::MC2*, and the average proportion of bilocular siliques per plant accounted for <40% (Figure 5k; Table S2), indicating that these plants could not restore a bilocular phenotype. *Mc2* expression was also analysed using qRT-PCR in the ovaries of these transgenic plants. Consistent with the complementation phenotype analyses, the higher the average proportion of bilocular siliques in these transgenic plants, the higher the *Mc2* transcription level in the ovary (Figure 5k), suggesting that *Mc2* expression in CMM is required for normal stem cell homeostasis.

In summary, when the *Mc2* promoter was truncated to –3511-bp from 5'–3', it did not affect *Mc2* expression in the CMM and would not increase the number of carpels in the silique. When it was truncated to –3467-bp, *Mc2* expression in CMM decreased, increasing the number of carpels in some siliques. When truncated to –3409-bp, *Mc2* expression in CMM was undetectable, increasing the number of carpels in more siliques and trilocular plant formation. Therefore, the –3512- to –3409-bp region of *Mc2* promoter was necessary for *Mc2* expression in CMM.

Phenotypes of null *mc2* alleles created by CRISPR-Cas9

As the 914-bp deletion of *Mc2* promoter in trilocular plants does not affect its expression in most tissues, to gain insight into its loss-of-function effects on IM and FM development, we generated several null alleles of *Mc2* gene using clustered regularly interspaced short palindromic repeats (CRISPR)/Cas9 genome editing, with two single guide sequences, S1 and S2; S1 was located in the upstream 599-bp promoter region, and S2 was located in the first exon 2077 bp of the coding region (Figure 2c). We obtained four lines with one- to seven-bp deletions in the protein-coding region that likely disrupted *Mc2* functionality (Figure 6a) from more than a hundred primary transformants. In all cases, the CR-*mc2* lines yielded fasciated inflorescences, flowers and siliques resembling the phenotype observed in *clv1-4*,

which is the strongest reported allele of *clv1* (Clark et al., 1993). The four loss-of-function alleles had the same phenotypes, and we chose line CR-*mc2-1*, which has a 4-bp deletion (nucleotide 2072–2075), for further experiments. Expression analysis using qRT-PCR revealed that *Mc2* was not expressed in CR-*mc2-1* (Figure 6b). Unlike *mc2* allele, the CR-*mc2-1* allele exhibited enlarged inflorescences (Figure 6c,d). The SEM results showed that in the CR-*mc2-1* flowers, the carpel primordium arose as a ring of organs around an enlarged and still-proliferating central dome at stage 5 (Figure 6e), at which time the FM terminated and carpel primordia arose at the centre of FM in wild-type flowers. In the later stages, this enlarged dome still appeared at the centre of gynoecium (Figure 6f–i). At stage 12, the cross-sectional observations showed a large mass of meristem tissue inside the gynoecium, which could generate an additional gynoecium (Figure 6j). This inner gynoecium can take up most of the space of the ovary, which caused the ovule and false septum to develop abnormalities in the CR-*mc2* lines (Figure 6j). During the flowering period, CR-*mc2-1* flowers showed an increase in the number of petals, stamens and carpels (Figure 6k,m, S2), and the gynoecium enlarged with the stigma cracked (Figure 6k,l).

Hence, our results revealed that null *mc2* alleles affected IM and FM development; the larger FM not only developed into a flower with additional organs in each whorl but also continued to proliferate and resulted a great mass of undifferentiated cells in the centre of the flower instead of terminating like the wild-type FM. Thus, in both the shoot and FM, null *mc2* alleles affected the balance between cell proliferation and differentiation.

Mc2 affecting the expression of genes involved in CMM development

As *Mc2* encodes an LRR-RLK, suggesting that it might perceive CLV3 or a related CLE peptide. In some plants, exogenous application of synthetic CLE peptides *in vitro* induced the consumption of meristems in the shoots and roots. *CLE26* could be expressed similarly to *Mc2* in CMM (Jun et al., 2010); therefore, we treated seedlings with peptides (CLV3 and CLE26) and measured the inhibition of root and epicotyl growth. Peptide treatment results showed that trilocular seedlings were the same as bilocular seedlings. Roots and epicotyls in seedlings treated with a control, scrambled CLV3 peptide (sCLV3) grew normally but were inhibited in the presence of CLV3 and CLE26 (Figure 7a, d). Further observation found that this inhibition was due to the restricted development of SAM (Figure 7b,e) and root apical meristem (RAM) (Figure 7c,f), indicating that *Mc2* functions in the SAM and RAM of trilocular seedlings, similar to that of bilocular seedlings. Furthermore, confocal microscopy revealed that the fluorescence expression of Mc2-GFP and Mc2-1-GFP showed plasma membrane localization in *Nicotiana benthamiana* epidermal cells (Figure S7), which is consistent with its proposed role as a membrane receptor (Stahl et al., 2013).

CLV1 is a major player in regulating the size of shoot apical, inflorescence and flower meristems. To better understand the molecular mechanisms in which *BjCLV1* regulates CMM development, we monitored the expression of genes involved in CLE peptide signalling genes, homeodomain TFs and CUP-SHAPED COTYLEDON (*CUC*) genes in ovaries from stage 8 flowers. The expression of the homolog of *WUS* (*BjA-WUS*, *BjuA001259*; *BjB-WUS*, *BjuB033714*) and a likely functional homolog of *CLV3* (*BjCLV3*, *BjuB026230*) was hardly detectable in the trilocular mutants and bilocular plants (Figure 7g), suggesting that *BjWUS*

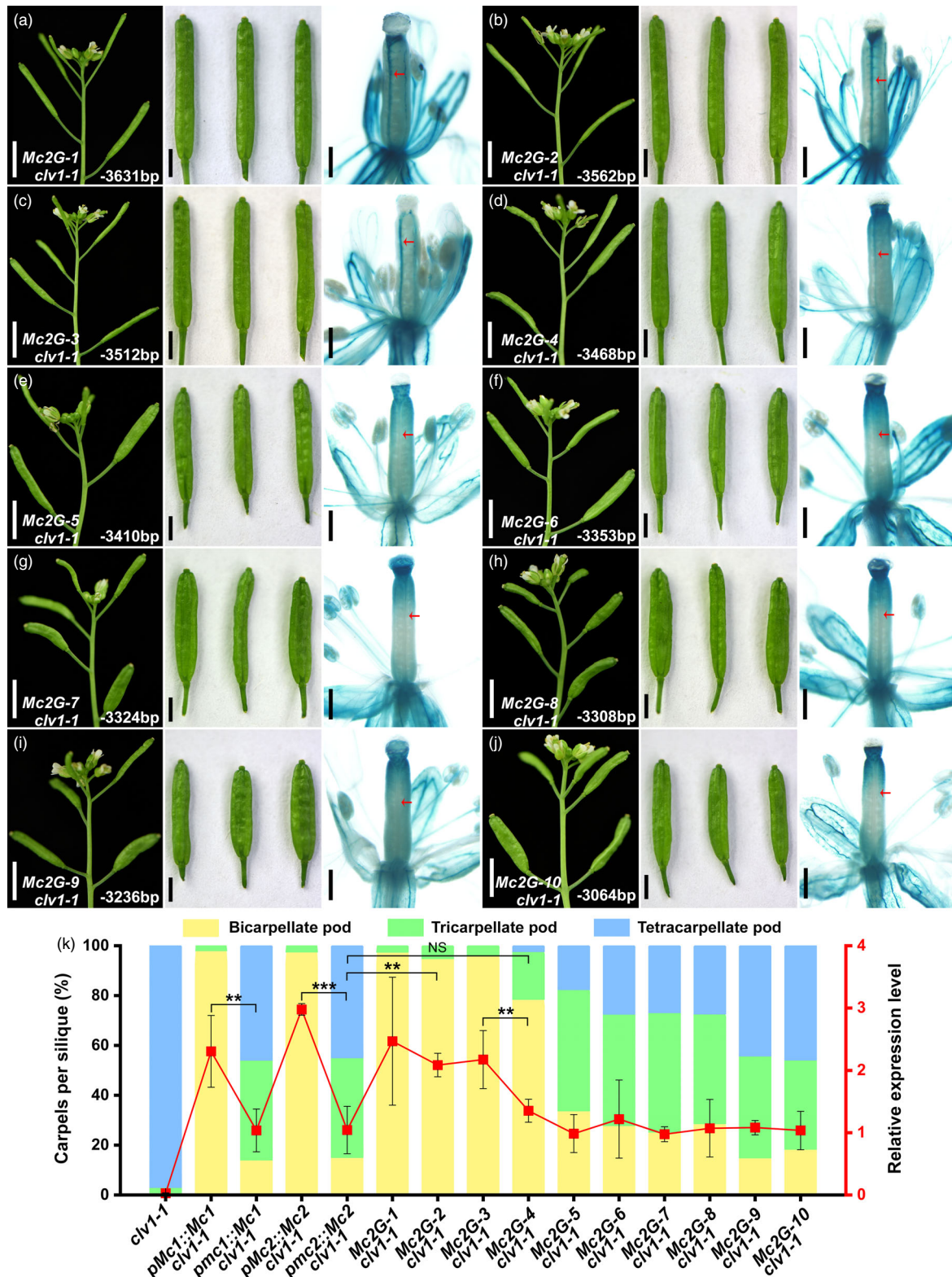


Figure 5 Promoter deletion analysis of *Mc2* in *Arabidopsis*. (a–j) The expression of complementary phenotype and analysis of GUS in gynoecium, containing different sections of *Mc2* promoter. The number indicates the relative distance from the 5' site of the section to *Mc2* gene translation initiator. (k) Quantification of carpel number (data are presented as average percentage of siliques per carpel number category; plant number per genotype = 20, silique number per plant >50) of indicated genotypes (T₁) and expression of *Mc1* or *Mc2* in the ovary from indicated genotypes detected using qRT-PCR. Error bars represent SD from three biological replicates. Significant differences by Student's *t*-test are shown as NS, not significant at $P \geq 0.05$; ** $P < 0.05$; *** $P < 0.001$. Scale bars = 5 mm, 2 mm, and 100 μ m for (a–j) (from left to right).

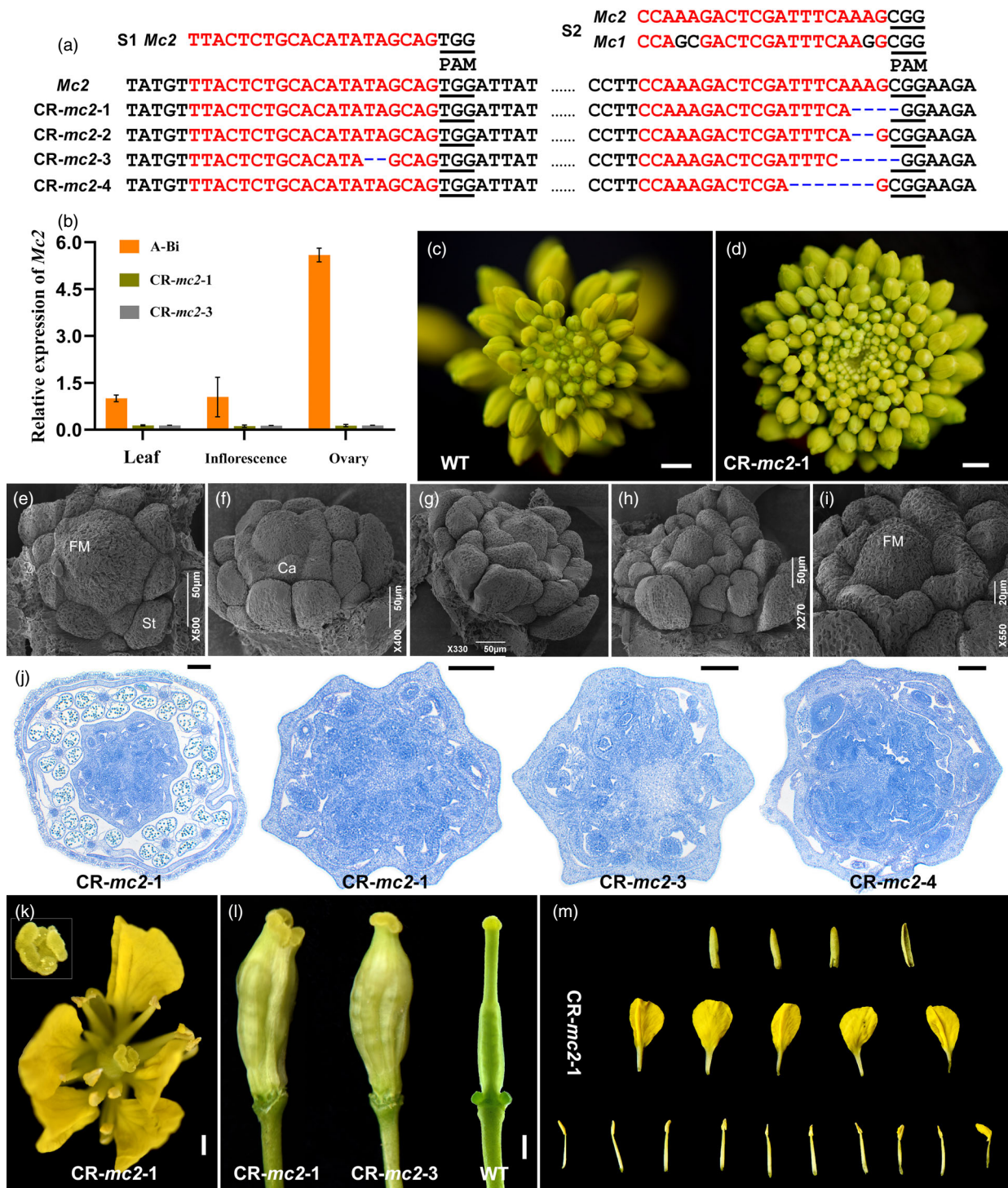


Figure 6 Phenotypes of the loss-of-function CRISPR/Cas9-*mc2* (CR-*mc2*) lines. (a) Loss-of-function CR-*mc2* alleles identified by cloning and sequencing PCR products from the *Mc2*-targeted region from four T₀ plants. Blue dashed lines indicate InDel mutations, and black bold and underlined letters indicate protospacer-adjacent motif (PAM) sequences. (b) Expression of *Mc2* in different tissues of two loss-of-function CR-*mc2* alleles and A-Bi, as revealed by qRT-PCR. Error bars indicate the SD of three replicates. (c, d) Inflorescence of the wild-type (WT) (c; A-Bi) and CR-*mc2*-1 (d). (e–i) Scanning electron microscopy images of CR-*mc2*-1 flowers at stages 5 (e), 6 (f) and 7 (g), and a gynoecium (i) from (h). (j) Cross sections for analysing the development of internal tissues of the gynoecium in the indicated alleles. (k) CR-*mc2*-1 flower; the box is the top view of the gynoecium, the stigma. (l) CR-*mc2*-1, CR-*mc2*-3 and WT (A-Bi) gynoecium. (m) CR-*mc2*-1 floral organs, including sepal, petal and stamen. Scale bars = 5 mm for (c) and (d), 200 μm for (j) and 1 mm for (k) and (l).

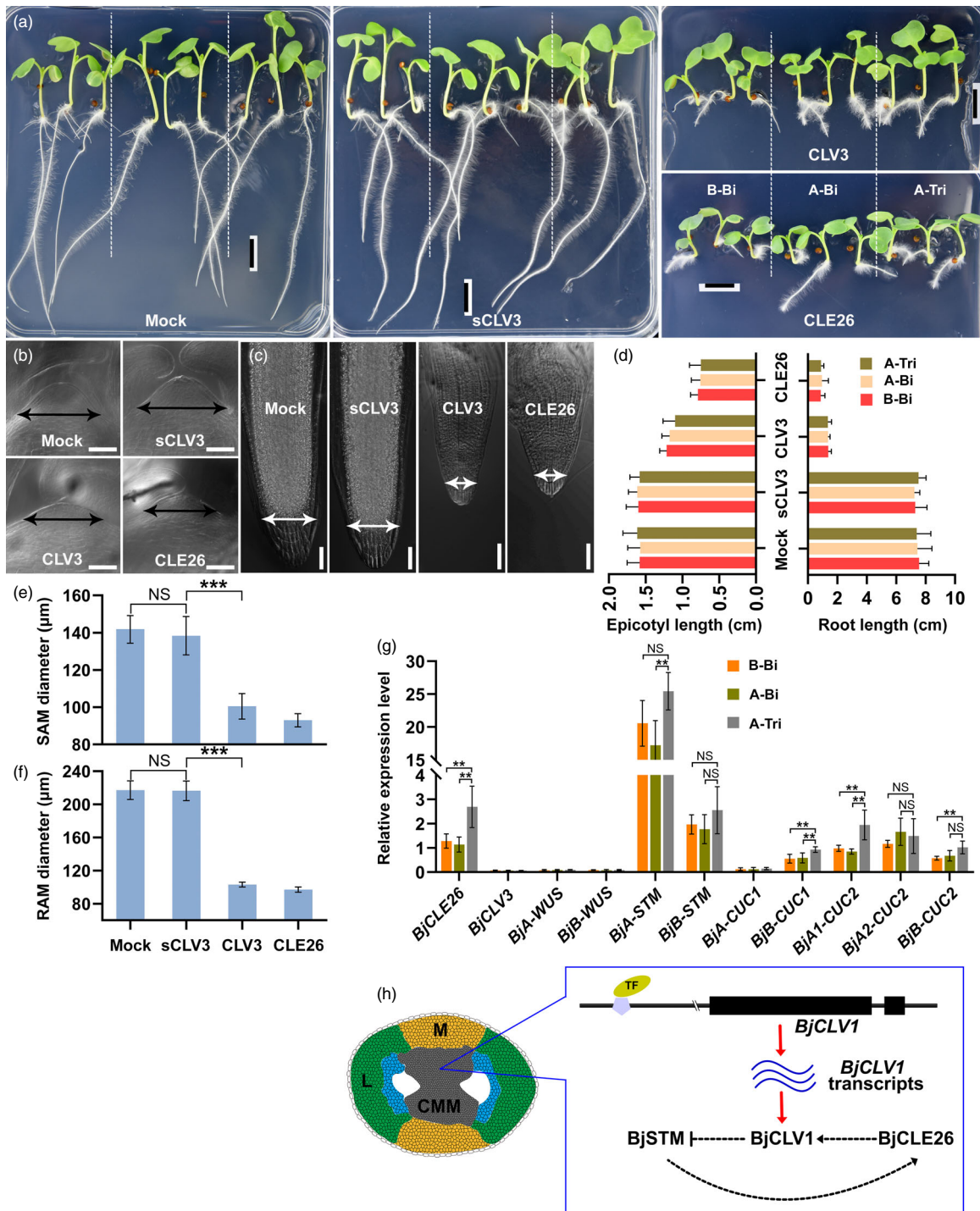


Figure 7 CLE peptide assays and pathway analysis. (a, d) Seven-day-old *Brassica juncea* seedlings were grown on agar media with or without the individual peptides; epicotyl and root length measurements are shown in (d). (b, e) Effect of different peptides on the shoot apical meristems (SAMs) of A-Tri (b); SAM diameter was quantified (e). (c, f) Effect of different peptides on the root apical meristems (RAMs) of A-Tri (c); RAM diameter was quantified (f). (g) Expression of *Arabidopsis* homologous genes involved in meristem maintenance and expressed in CMM in the ovary of the near-isogenic lines. The expression levels were determined using qRT-PCR and normalized to *Actin2*. The values are presented as the mean \pm SD ($n = 4$ biological replicates). (h) Proposed CMM maintenance via a feedback pathway containing the core receptor Mc2 in *Brassica juncea*. M, medial region; L, lateral region; CMM, carpel margin meristem; TF, transcription factor; the pentagram represents the core region, which may contain *cis*-regulatory specifically expressed in CMM. $n = 20$ for each genotype in (d), (e) and (f). Data in (d), (e) and (f) are presented as mean \pm SD. Significant differences by Student's *t*-test are shown as NS = not significant at $P \geq 0.05$; ** $P < 0.05$; *** $P < 0.001$. Scale bars = 1 cm for (a), 50 μm for (b) and 100 μm for (c).

and *BjCLV3* may not be the main factors in establishing and maintaining CMM. Notably, one additional *CLE* gene (*BjCLE26*, *BjuA027560*) was up-regulated in the trilocular mutants (Figure 7g). The expression of the homolog of *SHOOT MERISTEMLESS (STM)* (*BjA-STM*, *BjuA033384*; *BjB-STM*, *BjuB028275*) was increased in the trilocular mutants compared to that in the bilocular plants (Figure 7g), suggesting that *BjSTM* may control CMM size in the same pathway as *Mc2*. Furthermore, the expression of *BjCUC1* and *BjCUC2*, involved in shoot meristem initiation and required for formation and stable positioning of the CMMs in *Arabidopsis* (Kamiuchi et al., 2014), was significantly affected in the trilocular mutants. In the trilocular mutants, an increase expression of both genes was detected (Figure 7g), suggesting that *BjCUC1* and *BjCUC2* could also be involved in CMM formation during *B. juncea* gynoeceium development.

Discussion

The tissues and organs of *Arabidopsis* gynoeceium medial region, including the replum, placenta, septum, ovules and transmitting tract, are produced by CMM (Bowman et al., 1999); therefore, it is important to study the development mechanism of CMM to increase the Brassicaceae plant seed yield. In this study, we determined that trilocular silique formation was caused by CMM enlargement. There was a significant difference in CMM size between the bilocular and trilocular plants but no significant difference in the sizes of SAM, IM and FM. However, the SAM, IM and FM of multilocular plants were larger than those of bilocular plants in *B. rapa ml4* (Fan et al., 2014) and *B. juncea* 'duoshi' (Chen et al., 2018; Xiao et al., 2018). Thus, multilocular phenotype formation was concurrent with enlarged SAMs, which could lead to an enlarged FM and, further allowing the initiation of more floral organ primordia, with extra gynoeceium inside the silique as the FM failed to terminate. This showed that J163-4 was a natural weak mutant, which it will be more convenient to use, and the mechanism underlying trilocular silique formation differs from that of other multilocular plants.

In *Arabidopsis*, *CLV1* encodes a fully functional LRR-RLK, which plays a key role in shoot meristem maintenance (Clark et al., 1997; Stone et al., 1998). The *B. juncea* genome encodes two *CLV1* orthologs, *BjA7.CLV1* and *BjB3.CLV1*. In this study, we cloned another trilocular gene of J163-4, *mc2* and found a *CLV1* ortholog, *BjA7.CLV1*. Unlike *mc1*, whose transcription is interrupted by the insertion of the *BjB3.CLV1* coding region (Xu et al., 2017), there was no mutation in the coding region of *mc2*; however, there was a 914-bp deletion fragment in the promoter regulatory region, which did not affect the normal expression of *Mc2* in trilocular plants, except in the CMM. Therefore, when bilocular and trilocular seedlings were treated with *CLV3* peptides, *BjCLV1* located in SAM and RAM could receive *CLV3* peptide signals normally, thus inhibiting stem cell division, and seedlings showed stunted root and epicotyl growth (Figure 7a–f). However, both *Bjln1* and *Bjln2* in *B. juncea* 'duoshi' are homologous genes of *CLV1*. *Bjln1*, *BjA7.clv1*, is caused by a change in amino acids at positions 28 and 63 because of five SNPs in LRR domain of the coding region (Xiao et al., 2018), and *Bjln2* is caused by the insertion of a 4961-bp fragment in the coding region that interferes with the normal *BjB3.CLV1* transcription (Chen et al., 2018). This could explain why J163-4 and 'duoshi' have different phenotypes (Xiao et al., 2013; Xu et al., 2014), even though both have mutations in the *BjCLV1* gene. Gynoeceium cross sections have shown that a '+'-shaped false septum

divides the ovary into four locules in 'duoshi' (Xiao et al., 2013; Zhao, 2014), while trilocular siliques of J163-4 was divided into three locules by a 'll'-shaped false septum in this study. Furthermore, null *mc2* alleles developed more disorganized and fasciated siliques with low seed yield due to mutations in the coding region, leading to FM overproliferation. This suggests that compared to mutations in CDS of *BjCLV1* that alter protein structure, the *cis*-regulatory variant which affect the expression of *BjCLV1* in CMM only cause phenotypic change in siliques. Additionally, *ml4* (*tet-o*) of 'Yellow Sarson' and *srb* of 'Sangribai' in *B. rapa* are homologous genes of *CLV3*, and both are single-nucleotide mutations of *CLE* motif in the coding region and lead to amino acids changes (Fan et al., 2014; Yadava et al., 2014; Yang et al., 2021). Therefore, the J163-4 phenotype differs from that of other multilocular plants because of the different forms of mutation.

Conservatory analysis showed that the 914-bp deletion sequence of the *mc2* promoter had a relatively high level of conservation in Brassicaceae species (Figure 2d). The *BjCLV1* genome sequence with its complete promoter could rescue the *Bjclv1* and *clv1* mutant phenotype in *B. juncea* and *Arabidopsis*, respectively, while without the conserved deletion region of its promoter failed to rescue the mutant phenotype (Figure 3, S4). Similarly, promoters only including the 2691-, 2692-, 1945- or 2237-bp upstream regulatory sequence from TSS (Figure 2d), which the conserved deletion region, are not included, in the complementation constructs also partially rescue the mutant phenotype (Chen et al., 2018; Clark et al., 1997; Xiao et al., 2018; Xu et al., 2017). In contrast, *GUS* activity was detected in the CMM of gynoeceium when 3.4-kb upstream regulatory sequence (Figure 2d) containing the conserved deletion region was fused to the *GUS* reporter gene in transgenic *Arabidopsis* (Durbak and Tax, 2011). In addition, *Mc1* and *Mc2* mRNA were expressed in a broad range of *B. juncea* (Figure 4). This suggests that the collinearity segments of the 914-bp deletion sequence in the *CLV1* homologous promoter may contain *cis*-regulatory elements that affect their expression in CMM, and that *Mc1* and *Mc2* are a pair of functionally redundant genes that play vital roles in various tissues and organs of *B. juncea*. The *B. napus* genome also contains two *CLV1* homologous genes. Mutation of only one homologous gene will not lead to phenotypic change; a multilocular plant can only be obtained by knocking out two homologous genes simultaneously (Yang et al., 2018). The *CLV1* mRNA in *Arabidopsis* also constitutively expressed in diverse tissues (Clark et al., 1997; Dievart et al., 2003; Trotochaud et al., 1999). This conserved none-tissue-specific expression pattern suggested *CLV1* and *CLV1* orology are a conserved pleiotropy. Most functional studies of the *CLV1* gene have been performed in *Arabidopsis*, and genetic studies of *CLV1* homologs in other plants have shown conservation of meristem function (Somssich et al., 2016). Currently, it is known that uncovered pleiotropic roles of fruit-yield-related genes by generating CRISPR/Cas9 genome-edited promoter alleles in tomato and maize demonstrated that specific *cis*-regulatory regions control this pleiotropy (Hendelman et al., 2021; Liu et al., 2021; Rodríguez-Leal et al., 2017; Swinnen et al., 2016; Wang et al., 2021). This suggests that targeting the conserved *cis*-regulatory sequences of specially expressed *CLV1* orology in CMM mutations could produce multilocular siliques with higher yields in Brassicaceae crops.

From the phylogenetic tree, *CLV1* is highly conserved with at least one homolog in all Brassicaceae species (Figure 2d). This conserved evolutionary manner suggested a conserved receptor

function of BjCLV1 in *B. juncea* multiple meristems. Carpel development involves two key TFs, *STM* and *AGAMOUS* (*AG*) MADS box genes (Schofield *et al.*, 2007), which are activated in the centre of FM by the floral regular *LEAFY* (*LFY*) and the stem cell-promoting factor *WUS* in the early stages of flower development (Lenhard *et al.*, 2001; Lohmann *et al.*, 2001). After stage 6, *AG* directly represses *WUS* expression by binding to *WUS* locus and recruiting Polycomb Group (PcG) that methylates histone H3 Lys-27 at *WUS*, causing stem cell maintenance to terminate and thus permitting carpel development (Lenhard *et al.*, 2001; Liu *et al.*, 2011; Lohmann *et al.*, 2001). When the carpel primordia occupied the flower centre, no *WUS* or *CLV3* expression was detected (Lenhard *et al.*, 2001; Mayer *et al.*, 1998). Similarly, the expression of the homolog of *WUS* and *CLV3* was not detected in the *mc2* and bilocular ovaries (Figure 7g). The homeodomain TF *STM* is a key regulator of CMM development. *STM* is required for the formation and maintenance of SAM and is expressed in the CMM at the early stages of gynoecium development (Long *et al.*, 1996). Additionally, *CUC1* and *CUC2* are also required for the formation and stable positioning of CMMs, and between *CUC* and *STM* presence a positive feedback loop in CMM (Kamiuchi *et al.*, 2014; Spinelli *et al.*, 2011). Furthermore, *CLE26* can be expressed similarly to *Mc2* in CMM (Jun *et al.*, 2010). In this study, the expression of the homolog of *CLE26*, *STM* and *CUC* genes in the ovary was higher in *mc2* mutant than in bilocular plants, which may be because the expression of *BjSTM* in the OC of CMM, where it promotes stem cell division. *BjCLV1* is activated by peptide *BjCLE26*, which regulates *BjSTM* in a negative feedback loop, to restrict CMM stemness (Figure 7h). Therefore, loss of *BjCLV1* function in CMM leads to an expansion of the CMM, which leads to an increase in the number of CMMs and ultimately to trilocular silique formation. However, evidence of direct interaction between *Mc2* and *BjCLE26* and the TFs regulating *Mc2* expression in CMM are missing in this study; therefore, this will be the focus of our future studies. This did not affect our use of the excellent allele *mc2*. In breeding studies, we can utilize interspecific hybridization combined with molecular marker-assisted selection to transfer *mc2* into the widely planted *B. napus*; this is expected to breed more seeds per silique of high yield varieties of *B. napus* without affecting other traits.

In conclusion, the isolation and functional characterization of *CLV1* ortholog genes in *B. juncea* were reported. A novel 914-bp deletion fragment, which containing *cis*-regulatory elements was specifically expressed in CMM, in *BjA7*. *CLV1* promoter is essential for controlling CMM size and the number of locules and seeds per silique. Moreover, this *cis*-regulatory region is highly conserved in the promoter of *CLV1* ortholog genes in Brassicaceae, suggesting that this region can be edited to fine-tune CMM development without altering protein structure. These findings provide a new method for improving the seed yield-related traits in Brassicaceae crops.

Experimental procedures

Plant materials and growth conditions

Homozygous bilocular lines (A-Bi, genotype *mc1mc1Mc2Mc2*) and homozygous trilocular lines (A-Tri, genotype *mc1mc1mc2mc2*) from BC₇F₂ populations, which was constructed by using a trilocular line J163-4 and a bilocular line J268-1, were used for phenotypic and expression analyses of *Mc2*. Homozygous bilocular lines (B-Bi, genotype *Mc1Mc1mc2mc2*) and homozygous trilocular lines (B-Tri, genotype *mc1mc1mc2mc2*) from BC₆F₂

populations, which was constructed by using a trilocular line J163-4 and a bilocular line J248-2, were used for gene cloning and expression analysis of *Mc1*. *Brassica juncea* plants were grown at the experimental farm at Huazhong Agricultural University, Wuhan, China, in autumn. Transgenic *B. juncea* plants were grown in an isolated experimental station. *Arabidopsis* plants (*Col-0* ecotype, *Ler* ecotype and *clv1-1* mutant) were grown in a plant growth chamber at 20–22 °C and 70% humidity under a photoperiod of 16/8 h of light/dark.

Gene cloning and sequence analysis

The genomic DNA of *Mc2* (9118-bp, including 4827-bp upstream regulatory sequence from the translation start site (TSS) and 3043-bp coding region) and *mc2* (8204-bp, including 3913-bp upstream regulatory sequence from TSS and 3043-bp coding region) were amplified with specific primers (Table S3) and sequenced. To identify the *Mc2* homologous genes in Brassicaceae, BLAST analysis using the coding sequence (CDS) as a query was performed in BRAD database (<http://brassicadb.org/brad>). The most similar sequence was selected from each species. Sequence alignment and clustering of these homologs were performed with MEGA-X (<http://www.megasoftware.net>) using the neighbour-joining method with 1000 bootstrap replications. To determine whether 914-bp deletion sequence of *mc2* promoter has collinearity segments in *Mc2* homologous genes promoter region of Brassicaceae, BLAST analysis using 914-bp deletion sequence as a query was performed in BRAD database.

Plasmid construction and transformation

Four plasmids were constructed for complementation assay. Genomic DNA fragments of *Mc2* and *mc2*, including 3818-bp and 2864-bp upstream regulatory sequence from TSS, respectively, were amplified, respectively, cut with *EcoRI*/*KpnI* and cloned into pCAMBIA2300, generating *pMc2::Mc2* and *pmc2::Mc2* constructs. Genomic DNA fragments of *Mc1*, including 4581-bp and 2499-bp upstream regulatory sequence from TSS, respectively, were amplified, respectively, cut with *KpnI*/*PstI* and cloned into pCAMBIA2300, generating *pMc1::Mc1* and *pmc1::Mc1* constructs. To overexpress *Mc1* and *Mc2*, CDS for each was cloned into pCAMBIA2300 driven by two cauliflower mosaic virus 35S promoters, generating *p35S::Mc1* and *p35S::Mc2* constructs. To analyse the expression pattern of *Mc1* and *Mc2*, four promoter-reporter plasmids were constructed. The 4581-bp and 2499-bp upstream regulatory sequence from TSS of *Mc1* were amplified by PCR from B-Bi, respectively; the 3818-bp upstream regulatory sequence from TSS of *Mc2* was amplified by PCR from A-Bi; and 2864-bp upstream regulatory sequence from TSS of *mc2* was amplified by PCR from A-Tri and then fused to the gene for β-glucuronidase (*GUS*) reporter in the modified binary vector pCAMBIA2300 at *HindIII*/*BamHI* sites, respectively, generating *pMc1::GUS*, *pmc1::GUS*, *pMc2::GUS* and *pmc2::GUS* constructs. To identify the CMM-specific promoter region, ten promoter-reporter plasmids and ten complementary assay plasmids were constructed. The 3631-bp, 3562-bp, 3512-bp, 3468-bp, 3410-bp, 3353-bp, 3324-bp, 3308-bp, 3236-bp and 3064-bp upstream regulatory sequence from TSS of *Mc2* were amplified by PCR from A-Bi and then fused to the gene for *GUS* reporter in the modified binary vector pCAMBIA2300 at *HindIII*/*BamHI* sites, respectively, generating *GUS2-1*, *GUS2-2*, *GUS2-3*, *GUS2-4*, *GUS2-5*, *GUS2-6*, *GUS2-7*, *GUS2-8*, *GUS2-9* and *GUS2-10* constructs. And a series of genomic DNA fragments with 5'-deletion in the promoter of *Mc2*, including 3631-bp, 3562-bp,

3512-bp, 3468-bp, 3410-bp, 3353-bp, 3324-bp, 3308-bp, 3236-bp and 3064-bp upstream regulatory sequence from TSS, respectively, were amplified by PCR from A-Bi, cut with *KpnI*/*PstI* and cloned into pCambia2300, respectively, generating Mc2G-1, Mc2G-2, Mc2G-3, Mc2G-4, Mc2G-5, Mc2G-6, Mc2G-7, Mc2G-8, Mc2G-9 and Mc2G-10 constructs. Two knockout constructs, targeting *Mc2*, were produced. Two sequence-specific sgRNAs were designed using the web-based tool CRISPR-P (<http://crispr.hzau.edu.cn/CRISPR2>), one targeting the promoter region (S1) and one targeting the first exon (S2) for *Mc2*. Following a previously described method (Ma et al., 2015), two sgRNA cassettes driven by the promoters of AtU3d and AtU3b, respectively, were cloned into pYLCRISPR/Cas9P_{ubi}-H and pYLCRISPR/Cas9P_{35S}-H, in which Cas9p is driven by maize ubiquitin promoter (P_{ubi}) and cauliflower mosaic virus 35S promoter (P_{35S}), generating pMHMc2 and pDHMc2 constructs. The primers used for above plasmid construction were listed in Table S3. Finally, the constructed plasmids were introduced into *B. juncea* by Agrobacterium-mediated transformation using the hypocotyls infection method (Xu et al., 2017) or into *Arabidopsis* by Agrobacterium-mediated transformation using the floral dip method (Clough and Bent, 1998). The receptor plants used were listed in Table S4.

To investigate the subcellular localization of *Mc2*, CDS without the termination codon and CDS without the kinase domain were amplified from A-Bi using primers (Table S3). The amplified cDNA fragments were independently cloned into the pMDC83 vector at *KpnI*/*BamHI* site, to generate a C-terminal fusion with GFP under control of CaMV 35S promoter, generating *Mc2*-GFP and *Mc2*-1-GFP constructs.

Reverse-transcription PCR and qRT-PCR analysis

Total RNA was extracted from various plant tissues using RNeasy® Plant Mini Kit (QIAGEN, Chadstone Center, VIC, Australia) supplemented with RNase-free DNase I set to remove contaminating DNA according to the manufacturer's instructions. First-strand cDNA was synthesized using a RevertAid First Strand cDNA Synthesis Kit (Thermo, <http://www.thermofisher.com/cn/zh/home.html>). cDNA was amplified on a CFX96™ Real-time PCR Detection System (Bio-Rad, <http://bio-rad.com/>). *Actin2* gene was used as the internal controls for *B. juncea* and *Arabidopsis*. Quantitative RT-PCR measurements were obtained using relative quantification $2^{-\Delta\Delta C_t}$ method (Livak and Schmittgen, 2001). Data were expressed as the mean of three biological replicates \pm SD. The primer sequences were listed in Table S3.

In vitro peptide assay

sCLV3 (PPTRGLSHHPVD, scrambled peptide), CLV3 (RTVPSG PDLPHH) and CLE26 (RKVPRGPDPIHN) peptides with >95% purity were synthesized by Friendbio Science & Technology (Wuhan) Co., Ltd, Wuhan, China. The gel culture assay as described by Fan et al., (2014), *B. juncea* seeds were germinated on half MS gel medium overnight after surface-sterilized. Synchronized germinating seeds were selected and transferred to half MS gel medium containing sCLV3 (5 μ M) or CLV3, or CLE26 peptides in square plates placed vertically in a growth chamber. After 7 days, root and epicotyl length were measured, and RAM measurements were obtained using Image J (<https://imagej.net/>). The RAM diameter was defined by measuring the width of the root meristematic zone. The liquid culture assay as described by Fiers et al., (2006), *B. juncea* sterilized seeds were incubated in half MS liquid medium containing sCLV3 (5 μ M) or CLV3, or CLE26

peptides. The incubation was performed in 50 mL Falcon tubes (20 seeds/tube) containing 6 mL of medium on a roller bank. After 10 days, samples were collected, fixed and cleared, and SAM measurements were obtained using Image J. The SAM diameter was defined by measuring the width of the meristem where the first primordia were visible on each side.

Phenotype characterization, histochemical analysis and microscopy

Brassica juncea and *Arabidopsis* phenotype were photographed with a Nikon digital camera (D750). *Brassica juncea* gynoecium and *Arabidopsis* flower images were taken using an Olympus dissection microscope with an Olympus digital camera. Cross sections were performed as described by Fan et al., (2014). Photographs were captured with a Leica DM750 microscope with a Leica digital camera. Buds at different developmental stages were collected from A-Bi and A-Tri inflorescence and fixed in 2.5% glutaraldehyde in 0.1 M phosphate buffer (pH 7). The fixed samples were dehydrated with a graded ethanol series, dried using a critical point dryer (Leica, <https://www.leica-microsystems.com>), sputter-coated with gold (Nanotech SEMPRep II sputter coater) and images were taken under a JSM-6390 scanning electron microscope.

To measure the stem meristem size, the shoot apices of the embryos were excised under a dissecting microscope, cleared in Hoyer's solution as described by Fan et al., (2014), analysed by differential interference contrast microscopy and measured with Image J. The GUS staining was conducted by incubating various tissues or organs of transgenic plants in a solution containing 0.5 mg/mL X-Gluc at 37 °C overnight followed by washing three times with 70% ethanol (Jefferson et al., 1987). The stained tissues or organs were photographed under a stereomicroscope (Olympus SZX16, <https://www.olympus-ims.com/>).

Trait measurements

The number of primary branches per plant, number of siliquae per plant and plant height at physiological maturity were recorded in 15 competitive plants per genotype. After complete maturity, siliquae length, siliquae body length and number of seeds per siliquae were recorded in 30 competitive siliques per plant, and 1000-seed weight and seed yield per plant were recorded. The mean values of each genotype were subjected to statistical analysis.

Subcellular localization

Subcellular localization analysis was performed as described previously (Duan et al., 2020). Briefly, *A. tumefaciens* (GV3101) cells containing the desired constructs were co-infiltrated into four- to five-week-old *N. benthamiana* leaves using an infiltration buffer (10 mM MES, pH 5.7, 10 mM MgCl₂, and 150 μ M acetosyringone) to an OD₆₀₀ = 0.2. The infiltrated plants were left for 2 days. Samples of the infiltrated leaves were collected from the infected area and visualized using a confocal laser scanning microscope (Leica SP8). The excitation wavelengths for GFP and RFP were 488 and 543 nm, respectively.

Acknowledgements

The authors are grateful to Dr. Cilla Luo in New Zealand for critically reading the manuscript. This work was financially supported by the National Natural Science Foundation of China (NSFC, grant No. 31571698), the National Key Research and Development Program of China (grant No. 2016YFD0101300)

and the Program for Modern Agricultural Industrial Technology System of China (grant No. CARS-12).

Conflict of interest

The authors declare no conflict of interest.

Author contributions

JS and GW designed the experiments. GW performed most of the experiments and wrote the manuscript. XZ and PX constructed the mapping population. WH and ZL collected the phenotypic data. LZ, JW, BY, CM, JT and TF supervised this study. JS conceived and supervised the research and writing.

Data availability statement

The data that support the findings of this study are available from the corresponding author upon reasonable request.

References

- Bommert, P., Lunde, C., Nardmann, J., Vollbrecht, E., Running, M., Jackson, D., Hake, S. et al. (2005) *thick tassel dwarf1* encodes a putative maize ortholog of the *Arabidopsis* *CLAVATA1* leucine-rich repeat receptor-like kinase. *Development*, **132**, 1235–1245.
- Bowman, J.L., Baum, S.F., Eshed, Y., Putterill, J. and Alvarez, J. (1999) Molecular genetics of gynoecium development in *Arabidopsis*. *Curr. Top. Dev. Biol.*, **45**, 155–205.
- Brand, U., Fletcher, J.C., Hobe, M., Meyerowitz, E.M. and Simon, R. (2000) Dependence of stem cell fate in *Arabidopsis* on a feedback loop regulated by *CLV3* activity. *Science*, **289**, 617–619.
- Chen, C., Xiao, L.u., Li, X. and Du, D. (2018) Comparative mapping combined with map-based cloning of the *Brassica juncea* genome reveals a candidate gene for multilocular rapeseed. *Front. Plant Sci.*, **9**, 1744.
- Choudhary, B.R. and Solanki, Z.S. (2007) Inheritance of silique locule number and seed coat colour in *Brassica juncea*. *Plant Breeding*, **126**, 104–106.
- Clark, S.E., Running, M.P. and Meyerowitz, E.M. (1993) *CLAVATA1*, a regulator of meristem and flower development in *Arabidopsis*. *Development*, **119**, 397–418.
- Clark, S.E., Williams, R.W. and Meyerowitz, E.M. (1997) The *CLAVATA1* gene encodes a putative receptor kinase that controls shoot and floral meristem size in *Arabidopsis*. *Cell*, **89**, 575–585.
- Clough, S.J. and Bent, A.F. (1998) Floral dip: a simplified method for *Agrobacterium*-mediated transformation of *Arabidopsis thaliana*. *Plant J.*, **16**, 735–743.
- Dievart, A., Dalal, M., Tax, F.E., Lacey, A.D., Huttly, A., Li, J. and Clark, S.E. (2003) *CLAVATA1* dominant-negative alleles reveal functional overlap between multiple receptor kinases that regulate meristem and organ development. *Plant Cell*, **15**, 1198–1211.
- Duan, Z., Zhang, Y., Tu, J., Shen, J., Yi, B., Fu, T., Dai, C. et al. (2020) The *Brassica napus* GATA transcription factor BnA5.ZML1 is a stigma compatibility factor. *J. Integr. Plant Biol.*, **62**, 1112–1131.
- Durbak, A.R. and Tax, F.E. (2011) *CLAVATA* signaling pathway receptors of *Arabidopsis* regulate cell proliferation in fruit organ formation as well as in meristems. *Genetics*, **189**, 177–194.
- Fan, C., Wu, Y., Yang, Q., Yang, Y., Meng, Q., Zhang, K., Li, J. et al. (2014) A novel single-nucleotide mutation in a *CLAVATA3* gene homolog controls a multilocular silique trait in *Brassica rapa* L. *Mol. Plant*, **7**, 1788–1792.
- Fiers, M., Golemic, E., van der Schors, R., van der Geest, L., Li, K.W., Stiekema, W.J. and Liu, C.M. (2006) The *CLAVATA3*/ESR motif of *CLAVATA3* is functionally independent from the nonconserved flanking sequences. *Plant Physiol.*, **141**, 1284–1292.
- Fletcher, J.C., Brand, U., Running, M.P., Simon, R. and Meyerowitz, E.M. (1999) Signaling of cell fate decisions by *CLAVATA3* in *Arabidopsis* shoot meristems. *Science*, **283**, 1911–1914.
- Henkelman, A., Zebell, S., Rodriguez-Leal, D., Dukler, N., Robitaille, G., Wu, X., Kostyun, J. et al. (2021) Conserved pleiotropy of an ancient plant homeobox gene uncovered by *cis*-regulatory dissection. *Cell*, **184**, 1724–1739.
- Jefferson, R.A., Kavanagh, T.A. and Bevan, M.W. (1987) GUS fusions: β -glucuronidase as a sensitive and versatile gene fusion marker in higher plants. *EMBO J.*, **6**, 3901–3907.
- Jeong, S., Trotochaud, A.E. and Clark, S.E. (1999) The *Arabidopsis* *CLAVATA2* gene encodes a receptor-like protein required for the stability of the *CLAVATA1* receptor-like kinase. *Plant Cell*, **11**, 1925–1934.
- Jun, J., Fiume, E., Roeder, A.H., Meng, L., Sharma, V.K., Osmont, K.S., Baker, C. et al. (2010) Comprehensive analysis of *CLE* polypeptide signaling gene expression and overexpression activity in *Arabidopsis*. *Plant Physiol.*, **154**, 1721–1736.
- Kamiuchi, Y., Yamamoto, K., Furutani, M., Tasaka, M. and Aida, M. (2014) The *CUC1* and *CUC2* genes promote carpel margin meristem formation during *Arabidopsis* gynoecium development. *Front. Plant Sci.*, **5**, 165.
- Katiyar, R.K., Chamola, R. and Chopra, V.L. (1998) Tetralocular mustard, *Brassica juncea*: new promising variability through interspecific hybridization. *Plant Breeding*, **117**, 398–399.
- Lenhard, M., Bohnert, A., Jürgens, G. and Laux, T. (2001) Termination of stem cell maintenance in *Arabidopsis* floral meristems by interactions between *WUSCHEL* and *AGAMOUS*. *Cell*, **105**, 805–814.
- Liu, L., Gallagher, J., Arevalo, E.D., Chen, R., Skopelitis, T., Wu, Q., Bartlett, M. et al. (2021) Enhancing grain-yield-related traits by CRISPR-Cas9 promoter editing of maize *CLE* genes. *Nat. Plants*, **7**, 287–294.
- Liu, X., Kim, Y.J., Müller, R., Yumul, R.E., Liu, C., Pan, Y., Cao, X. et al. (2011) *AGAMOUS* terminates floral stem cell maintenance in *Arabidopsis* by directly repressing *WUSCHEL* through recruitment of Polycomb Group proteins. *Plant Cell*, **23**, 3654–3670.
- Livak, K.J. and Schmittgen, T.D. (2001) Analysis of relative gene expression data using real-time quantitative PCR and the $2^{-\Delta\Delta CT}$ method. *Methods*, **25**, 402–408.
- Lohmann, J.U., Hong, R.L., Hobe, M., Busch, M.A., Parcy, F., Simon, R. and Weigel, D. (2001) A molecular link between stem cell regulation and floral patterning in *Arabidopsis*. *Cell*, **105**, 793–803.
- Long, J.A., Moan, E.I., Medford, J.I. and Barton, M.K. (1996) A member of the *KNOTTED* class of homeodomain proteins encoded by the *STM* gene of *Arabidopsis*. *Nature*, **379**, 66–69.
- Lv, Z., Xu, P., Zhang, X., Wen, J., Yi, B., Ma, C., Tu, J. et al. (2012) Primary study on anatomic and genetic analyses of multi-loculus in *Brassica juncea*. *Chinese J. Oil Crop Sci.*, **34**, 461–466.
- Ma, X., Zhang, Q., Zhu, Q., Liu, W., Chen, Y., Qiu, R., Wang, B. et al. (2015) A robust CRISPR/Cas9 system for convenient, high-efficiency multiplex genome editing in monocot and dicot plants. *Mol. Plant*, **8**, 1274–1284.
- Mayer, K.F., Schoof, H., Haecker, A., Lenhard, M., Jürgens, G. and Laux, T. (1998) Role of *WUSCHEL* in regulating stem cell fate in the *Arabidopsis* shoot meristem. *Cell*, **95**, 805–815.
- Reyes-Olalde, J.I., Zuniga-Mayo, V.M., Chavez-Montes, R.A., Marsch-Martinez, N. and de Folter, S. (2013) Inside the gynoecium: at the carpel margin. *Trends Plant Sci.*, **18**, 644–655.
- Rodríguez-Leal, D., Lemmon, Z.H., Man, J., Bartlett, M.E. and Lippman, Z.B. (2017) Engineering quantitative trait variation for crop improvement by genome editing. *Cell*, **171**, 470–480.
- Schoof, H., Lenhard, M., Haecker, A., Mayer, K.F.X., Jürgens, G. and Laux, T. (2000) The stem cell population of *Arabidopsis* shoot meristems is maintained by a regulatory loop between the *CLAVATA* and *WUSCHEL* genes. *Cell*, **100**, 635–644.
- Scotfield, S., Dewitte, W. and Murray, J.A. (2007) The *KNOX* gene *SHOOT MERISTEMLESS* is required for the development of reproductive meristematic tissues in *Arabidopsis*. *Plant J.*, **50**, 767–781.
- Smyth, D.R., Bowman, J.L. and Meyerowitz, E.M. (1990) Early flower development in *Arabidopsis*. *Plant Cell*, **2**, 755–767.
- Somssich, M., Je, B.I., Simon, R. and Jackson, D. (2016) *CLAVATA*-*WUSCHEL* signaling in the shoot meristem. *Development*, **143**, 3238–3248.
- Spinelli, S.V., Martin, A.P., Viola, I.L., Gonzalez, D.H. and Palatnik, J.F. (2011) A mechanistic link between *STM* and *CUC1* during *Arabidopsis* development. *Plant Physiol.*, **156**, 1894–1904.

- Stahl, Y., Grabowski, S., Bleckmann, A., Kühnemuth, R., Weidtkamp-Peters, S., Pinto, K., Kirschner, G. et al. (2013) Moderation of *Arabidopsis* root stemness by CLAVATA1 and ARABIDOPSIS CRINKLY4 receptor kinase complexes. *Curr. Biol.*, **23**, 362–371.
- Stone, J.M., Trotochaud, A.E., Walker, J.C. and Clark, S.E. (1998) Control of meristem development by CLAVATA1 receptor kinase and kinase-associated protein phosphatase interactions. *Plant Physiol.*, **117**, 1217–1225.
- Suzaki, T., Sato, M., Ashikari, M., Miyoshi, M., Nagato, Y. and Hirano, H.Y. (2004) The gene *FLORAL ORGAN NUMBER1* regulates floral meristem size in rice and encodes a leucine-rich repeat receptor kinase orthologous to *Arabidopsis* CLAVATA1. *Development*, **131**, 5649–5657.
- Swinnen, G., Goossens, A. and Pauwels, L. (2016) Lessons from domestication: targeting *cis*-regulatory elements for crop improvement. *Trends Plant Sci.*, **21**, 506–515.
- Trotochaud, A.E., Hao, T., Wu, G., Yang, Z. and Clark, S.E. (1999) The CLAVATA1 receptor-like kinase requires CLAVATA3 for its assembly into a signaling complex that includes KAPP and a Rho-related protein. *Plant Cell*, **11**, 393–406.
- Wang, G., Zhang, X., Xu, P., Lv, Z., Wen, J., Yi, B., Ma, C. et al. (2016) Fine mapping of polycyclic gene (*Bjmc2*) in *Brassica juncea* L. *Acta Agronomica Sinica*, **42**, 1735–1742.
- Wang, X., Aguirre, L., Rodríguez-Leal, D., Hendelman, A., Benoit, M. and Lippman, Z.B. (2021) Dissecting *cis*-regulatory control of quantitative trait variation in a plant stem cell circuit. *Nat. Plants*, **7**, 419–427.
- Xiao, L.u., Li, X., Liu, F., Zhao, Z., Xu, L., Chen, C., Wang, Y. et al. (2018) Mutations in the CDS and promoter of *BjuA07.CLV1* cause a multilocular trait in *Brassica juncea*. *Sci. Rep.*, **8**, 5339.
- Xiao, L.u., Zhao, H., Zhao, Z., Du, D., Xu, L., Yao, Y., Zhao, Z. et al. (2013) Genetic and physical fine mapping of a multilocular gene *Bjln1* in *Brassica juncea* to a 208-kb region. *Mol. Breeding*, **32**, 373–383.
- Xu, C., Liberatore, K.L., MacAlister, C.A., Huang, Z., Chu, Y.-H., Jiang, K.e., Brooks, C. et al. (2015) A cascade of arabinosyltransferases controls shoot meristem size in tomato. *Nat. Genet.*, **47**, 784–792.
- Xu, P., Cao, S., Hu, K., Wang, X., Huang, W., Wang, G., Lv, Z. et al. (2017) Trilocular phenotype in *Brassica juncea* L. resulted from interruption of *CLAVATA1* gene homologue (*BjMc1*) transcription. *Sci. Rep.*, **7**, 3498.
- Xu, P., Lv, Z., Zhang, X., Wang, X., Pu, Y., Wang, H., Yi, B. et al. (2014) Identification of molecular markers linked to trilocular gene (*mc1*) in *Brassica juncea* L. *Mol. Breeding*, **33**, 425–434.
- Yadav, R.K., Perales, M., Gruel, J., Girke, T., Jonsson, H. and Reddy, G.V. (2011) WUSCHEL protein movement mediates stem cell homeostasis in the *Arabidopsis* shoot apex. *Genes Dev.*, **25**, 2025–2030.
- Yadava, S.K., Paritosh, K., Panjabi-Massand, P., Gupta, V., Chandra, A., Sodhi, Y.s., Pradhan, A.K. et al. (2014) Tetralocular ovary and high silique width in yellow sarson lines of *Brassica rapa* (subspecies *trilocularis*) are due to a mutation in *Bra034340* gene, a homologue of *CLAVATA3* in *Arabidopsis*. *Theor. Appl. Genet.*, **127**, 2359–2369.
- Yang, J., Liu, D., Wang, X., Ji, C., Cheng, F., Liu, B., Hu, Z. et al. (2016) The genome sequence of allopolyploid *Brassica juncea* and analysis of differential homoeolog gene expression influencing selection. *Nat. Genet.*, **48**, 1225–1232.
- Yang, Y., Li, H., Hu, L., Fan, C. and Zhou, Y. (2021) Genetic analysis and molecular characterization of multilocular trait in the *srb* mutant of *Brassica rapa* L. *Acta Agronomica Sinica*, **47**, 385–393.
- Yang, Y., Zhu, K., Li, H., Han, S., Meng, Q., Khan, S.U., Fan, C. et al. (2018) Precise editing of *CLAVATA* genes in *Brassica napus* L. regulates multilocular silique development. *Plant Biotechnol. J.*, **16**, 1322–1335.
- Zhao, H. (2014) *Fine mapping of multilocular gene Bjln1 in Brassica juncea* L. MS thesis, Qinghai University, Wuhan, China.
- Zhao, H., Du, D., Liu, Q., Li, X., Yu, Q. and Fu, Z. (2003) Performance in main characteristics of multilocular *Brassica juncea*. *Acta Agric. Boreali-occident. Sinica*, **12**, 62–64.

Supporting information

Additional supporting information may be found online in the Supporting Information section at the end of the article.

Figure S1 Shoot apical meristems and the floral phenotype of bilocular and trilocular plants in A-Bi and A-Tri lines.

Figure S2 Average numbers of *Brassica juncea* floral organs in indicated genotypes.

Figure S3 Transgenic plants (T_0) obtained in the overexpression and complementation experiment and quantification of carpel number in indicated genotypes of *Brassica juncea* (T_1).

Figure S4 Complementation test of *Mc1* and *Mc2* in *Arabidopsis*.

Figure S5 Activity differences in the normal and mutant promoter of *Mc1* and *Mc2* gene during reproductive growth.

Figure S6 Schematic representation of the constructs that expressed *Mc2*, driven by ten truncated promoters.

Figure S7 Subcellular localization of *Mc2*.

Table S1 Gene annotations in the *Mc2* candidate region.

Table S2 Quantification of carpel number in the indicated genotypes of *Arabidopsis*.

Table S3 Primers used in this study.

Table S4 The receptor plants used in the constructed plasmids transformation.